INTEGRATION OF EAVES AND SHADING DEVICES FOR IMPROVING THE THERMAL COMFORT IN A MULTI-ZONE BUILDING

by

Muhammad Abdalkhalaq Chuayb HADDAM [a], ***Sidi Mohammed El Amine BEKKOUCHE*** [b*], ***Tayeb BENOUAZ*** [a], ***Maamar HAMDANI*** [b], ***Mohamed Kamel CHERIER*** [b], ***and Noceir BENAMRAN*** [b]

[a] University of Tlemcen, Tlemcen, Algeria
[b] Applied Research Unit on Renewable Energies, (URAEA), Renewable Energy Development Center, (CDER), Ghardaia, Algeria

Original scientific paper
DOI: 10.2298/TSCI140422117H

This paper introduces a new approach to the description and modelling of multi-zone buildings in Saharan climate. Therefore, nodal method was used to apprehend thermo-aeraulic behavior of air subjected to varied solicitations. A coupling was made between equations proposed by P. Rumianowski and some equations of a building thermal energy model found in the TRNSYS user manual. Runge-Kutta fourth order numerical method was used to solve the obtained system of differential equations.
Theses results show that proper design of passive houses in an arid region is based on the control of direct solar gains, temperatures, and specific humidities. According to the compactness index, the insertion of solar shading and eaves can provide improved thermo-aeraulic comfort.

Key words: *eaves, solar shading, temperature, specific humidity, multi-zone model*

Introduction

Building simulation has developed rapidly since the 1960. It is a very important tool to analyze and predict the thermal performance and energy consumption of buildings. Modelling is a trade-off between reliability, accuracy, and time. Using software packages in the building environmental engineering field, simulations of building thermal performance are increasingly being used to address real world problems in the design of energy efficient buildings and healthy buildings. Heat, air, and moisture models describe combined heat, air, and moisture transfer in building components. The models differ in the way the transfer phenomena are modelled [1].

Two kinds of mathematical methods are used in the simulation of building thermal performance: first is frequency domain method, such as Fourier transformation, which requires the harmonic decomposition of all heat disturbances with fast Fourier transformation technique and the second is time domain method, such as transfer function [2], thermal response factors *Z-transform function* [3], nodal method *finite volume* [4], state space method [5]. To date,

* Corresponding author; e-mail: smabekkouche@yahoo.fr

SIMBAD [6] has several building models that are mono-zone models. When the user needs to simulate a multi-zone building, he had to break it down to several mono-zone blocks and to couple them manually. However, to explain the model separation approach, Fanger [7] has identified the dominant modes of heat transfer that need to be described adequately to quantify a building's energy consumption and the occupant's thermal comfort.

It is well known that the building envelope is one of the most affecting factors in the energy consumption of buildings. The study of surface temperatures of walls is not of purely academic interest, but a step forward to the comprehension of the building behavior, the improvement of the building envelope, and the prediction of comfort levels inside it. Massive walls (concrete, brick, *etc*.) are time-dependent in nature, and cannot be modeled by a simple R-value, yet this is what is commonly done leading to inaccurate computer modeling, and incorrect estimation of energy loads. When a particular configuration for the external and internal walls of a building must be studied for a certain climate, there is a wide variety of thermal analysis that can be used to characterize the wall thermal behavior under these outdoor conditions [8].

Various numerical modelling approaches have been used to predict detailed information within the indoor environment. The type of approach used depends on the complexity of the phenomena observed, the results expected, the parameters investigated, and the degree of required accuracy. Cartes [9] stress the importance of creating common patterns of design for a better performances achievement of buildings, owing to the fact that traditional models have been inherited and already exist as valid references. The proposed multi-zone model can easily handle hundreds of zones simultaneously.

Otherwise, in a real building, the instantaneous solar gains are either used to supply part of the losses, or stored in the building structure for later use. Some part of the solar gains is not useful, since they overheat the air. Monsen *et al*. [10] present a more general design method for direct gain systems. In this paper a simplified method for calculating the solar gain is presented. It shows also the adaptation of a method of thermal analysis, the nodal analysis, linked to the case of building's thermal behaviour. We take successively an interest in the case of conduction into a wall, in the coupling with superficial exchanges and finally in the constitution of thermal models of the building. The study was performed for the air and walls of a residence for Applied Research Unit on Renewable Energies. The transient thermal behavior, especially the temperature of the air, and walls was monitored during one summer week. The fitting with the thermal behavior predicted by this method is discussed. In this contribution, thermal nodal method was used to apprehend thermal behavior of air subjected to varied solicitations. The nodal analysis is a powerful method of investigation in the thermal analysis of systems. It has been used in several branches such as solar energy systems [11], micro-electronics [12] or also the spatial field [13]. We will gradually use this approach in the domain of building's physics and we'll interest ourselves in the automatic generation of nodal models.

Multi-zone building modeling: mass and enthalpy balances

One of the fundamental laws of physics states that mass can neither be produced nor destroyed, *i*. *e*. mass is conserved. Although energy can change in form, it can not be created or destroyed. These two laws of physics provide the basis for two tools which are used routinely in environmental engineering and science *the mass balance and the enthalpy balance*, knowing that the enthalpy is a measure of the total energy of a thermodynamic system.

Enthalpy balance

Assuming that an area Zone *i* is in contact with $N + 1$ other zone, outside is represented by area N° 0. For the Zone *i*, the enthalpy change per unit time is written by the equation [14]:

$$\frac{\mathrm{d}H(i)}{\mathrm{d}t} = H^{\mathrm{e}}(i) - H^{\mathrm{leav}}(i) + \sum_{j=i}^{NW(i)} S_j h_{\mathrm{cij}}[T_{\mathrm{sij}}(i) - T_{\mathrm{al}}(i)] + P_{\mathrm{L}} + P_{\mathrm{s}} + CI_{\mathrm{L}} + CI_{\mathrm{s}} \quad (1)$$

$$H^{\mathrm{e}}(i) = \sum_{n=0}^{N} Q_{\mathrm{mas}}^{\mathrm{trans}}(n,i)[T_{\mathrm{al}}(n)C_{\mathrm{as}} + r_{\mathrm{s}}(n)][L_{\mathrm{v}} + C_{\mathrm{v}}T_{\mathrm{al}}(n)] \quad (2)$$

$$H^{\mathrm{leav}}(i) = \sum_{n=0}^{N} Q_{\mathrm{mas}}^{\mathrm{trans}}(i,n)[T_{\mathrm{al}}(i)C_{\mathrm{as}} + r_{\mathrm{s}}(i)][L_{\mathrm{v}} + C_{\mathrm{v}}T_{\mathrm{al}}(i)] \quad (3)$$

where $\sum_{j=i}^{NW(i)} S_{\mathrm{j}} h_{\mathrm{cij}}[T_{\mathrm{sij}}(i) - T_{\mathrm{al}}(i)]$ are expressions of the convective flow exchange between surfaces j of walls for Zone i corresponding to a temperature T_{sij} and the air mass in this zone corresponding to a temperature T_{al} (W) [15].

Expression of convective transfer coefficients due to exchange between the air and walls inner surfaces are given in [16].

Mass balance of dry air

In the building thermal, temporal variations in mass are very low amounts, which allow simplification of the conservation equation of air mass in Zone i [14]:

$$\sum_{n=0}^{N} Q_{\mathrm{mas}}^{\mathrm{trans}}(n,i) - Q_{\mathrm{mas}}^{\mathrm{trans}}(i,n) = \frac{\mathrm{d}m_{\mathrm{as}}}{\mathrm{d}t} \approx 0 \Rightarrow \sum_{n=0}^{N} Q_{\mathrm{mas}}^{\mathrm{trans}}(n,i) = \sum_{n=0}^{N} Q_{\mathrm{mas}}^{\mathrm{trans}}(i,n) \quad (4)$$

This equation reflects that the sum of the mass flows of dry air entering the Zone i is equal to the sum of the mass flows leaving the Zone i. This equation allows us, hereinafter, to simplify the writing of enthalpy balances.

Enthalpy changes: sensible and latent balance

An enthalpy change describes the change in enthalpy observed in the constituents of a thermodynamic system when undergoing a transformation or chemical reaction [17]:

$$H(i) = H_{\mathrm{s}}(i) + H_{\mathrm{L}}(i) = m_{\mathrm{as}}C_{\mathrm{as}}T_{\mathrm{al}}(i) + m_{\mathrm{as}}r_{\mathrm{s}}(i)[L_{\mathrm{v}} + C_{\mathrm{v}}T_{\mathrm{al}}(i)] \quad (5)$$

We can neglect $m_{\mathrm{as}}C_{\mathrm{v}}T_{\mathrm{al}}(i)$ if we compare this amount with $m_{\mathrm{as}}r_{\mathrm{s}}(i)L_{\mathrm{v}}$, $L_{\mathrm{v}} = 2500$ kJ/kg and $C_{\mathrm{v}} = = 1.96$ kJ/kgK. Therefore,

$$H_{\mathrm{s}}(i) \approx m_{\mathrm{as}}C_{\mathrm{as}}T_{\mathrm{al}}(i) \quad (6)$$

$$H_{\mathrm{L}}(i) \approx m_{\mathrm{as}}r_{\mathrm{s}}(i)L_{\mathrm{v}} \quad (7)$$

This helps to write the eq. (8) [14]:

$$\frac{\mathrm{d}H(i)}{\mathrm{d}t} = \frac{\mathrm{d}H^{\mathrm{e}}(i)}{\mathrm{d}t} - \frac{\mathrm{d}H^{\mathrm{leav}}(i)}{\mathrm{d}t} \quad (8)$$

This simplification allows us to write two equations of enthalpy balance: sensible balance, as a function only of $T_{\mathrm{al.}}$ and latent balance, as a function only of r_{s}. As we have already mentioned, in the building thermal, temporal variations in mass are very low amounts, the change in enthalpy can be assimilated to the variation in temperature:

$$\frac{\mathrm{d}H_{\mathrm{s}}(i)}{\mathrm{d}t} = \frac{d(m_{\mathrm{as}}C_{\mathrm{as}}T_{\mathrm{al}}(i))}{\mathrm{d}t} = C_{\mathrm{as}}\frac{\mathrm{d}m_{\mathrm{as}}}{\mathrm{d}t}T_{\mathrm{al}}(i) + C_{\mathrm{as}}\frac{\mathrm{d}T_{\mathrm{al}}(i)}{\mathrm{d}t}m_{\mathrm{as}} \tag{9}$$

$$\frac{\mathrm{d}H_{\mathrm{s}}(i)}{\mathrm{d}t} = H_{\mathrm{s}}^{\mathrm{e}}(i) - H_{\mathrm{s}}^{\mathrm{leav}}(i) + \sum_{j=i}^{NW(i)} S_{\mathrm{j}}h_{\mathrm{cij}}[T_{\mathrm{sij}}(i) - T_{\mathrm{al}}(i)] + P_{\mathrm{s}} + CI_{\mathrm{s}} \tag{10}$$

From this result, the following equation was obtained for the temperature function [14]:

$$\rho_{\mathrm{as}}C_{\mathrm{as}}V(i)\frac{\mathrm{d}T_{\mathrm{al}}(i)}{\mathrm{d}t} = \sum_{i=0}^{N}\{Q_{\mathrm{mas}}^{\mathrm{trans}}(i,n)C_{\mathrm{as}}[T_{\mathrm{al}}(n) - T_{\mathrm{al}}(i)]\} + \sum_{j=i}^{NW(i)}[S_{\mathrm{j}}h_{\mathrm{cij}}\{T_{\mathrm{sij}}(i) - T_{\mathrm{al}}(i)]\} + P_{\mathrm{s}} + CI_{\mathrm{s}} \tag{11}$$

We obtain a system of N equations with N unknowns, the main variables are the air temperatures in each zone. The surface temperature T_{sij} will be obtained by establishing thermal balance of the wall inner surface. It is through these balances that we see couplings with other modes of heat transfer. In the same manner as the sensible balance, neglecting the term $\mathrm{d}m_{\mathrm{as}}/\mathrm{d}t$, and with using the simplified conservation equation of the dry air mass, we get the eq. (15):

$$\frac{H_{\mathrm{L}}(i)}{\mathrm{d}t} = H_{\mathrm{L}}^{\mathrm{e}}(i) - H_{\mathrm{L}}^{\mathrm{leav}}(i) + P_{\mathrm{L}} + CI_{\mathrm{L}} \tag{12}$$

$$m_{\mathrm{as}}(i) = \frac{V(i)}{v_{\mathrm{s}}(i)} \tag{13}$$

$$\frac{\mathrm{d}H_{\mathrm{L}}(i)}{\mathrm{d}t} = \frac{d(m_{\mathrm{as}}r_{\mathrm{s}}(i)Lv)}{\mathrm{d}t} = Lv\frac{\mathrm{d}m_{\mathrm{as}}}{\mathrm{d}t}r_{\mathrm{s}}(i) + Lv\frac{\mathrm{d}r_{\mathrm{s}}(i)}{\mathrm{d}t}m_{\mathrm{as}} \tag{14}$$

$$m_{\mathrm{as}}(i)\frac{\mathrm{d}r_{\mathrm{s}}(i)}{\mathrm{d}t} = \sum_{i=0}^{N}\{Q_{\mathrm{mas}}^{\mathrm{trans}}(i,n)[r_{\mathrm{s}}(n) - r_{\mathrm{s}}(i)]\} + \frac{P_{\mathrm{L}}}{L_{\mathrm{v}}} + \frac{CI_{\mathrm{L}}}{L_{\mathrm{v}}} \tag{15}$$

As for the sensitive balance, a system of N equations with N unknowns is obtained, the main variables are the specific humidities in each zone [14].

We can use the empirical formulas of Nadeau and Puiggali [18] and specific humidity may be expressed as a function of relative humidity by the relationship:

$$H_{\mathrm{s}} = \frac{0.622P_{\mathrm{sat}}(T)Hr}{101325 - P_{\mathrm{sat}}(T)Hr} \tag{16}$$

$$P_{\mathrm{sat}}(T) = \mathrm{e}^{23.3268 - \frac{3802.7}{T} - \left[\frac{472.68}{T}\right]^2} \tag{17}$$

Heat conduction model and coupling with superficial exchanges

For an envelope's wall, and in the hypothesis of mono-dimensional conductive transfers, the transposition of the thermal problem of conduction into an electrical problem is called thermo-electrical analogy. The nodes, which in an electrical meaning symbolize equipotentials, correspond to isotherm lines. Therefore, each of those nodes is getting an electrical capacitor, traducing the thermal storage of the corresponding wall's part, and allowing in this the traduction of the thermal inertia effects. In this section, we propose a simplified approach allows representing the multilayer system by a model based on an electrical analogy proposed by Rumianowski *et al*. [19] and then it was taken by Con *et al*. in 2003 It is often used when we are

interested to the determination of the temperature of any node inside a wall. The conduction model is given in detail in references [16, 19, 20].

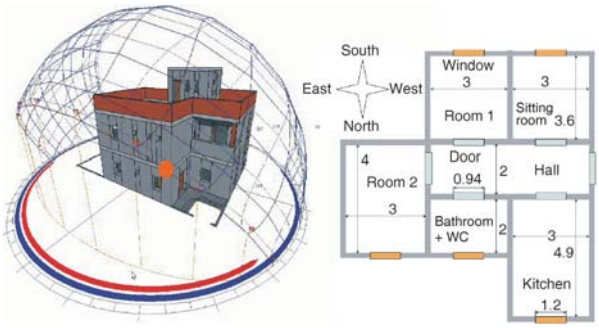

Figure 1. Diagram, solar path and descriptive plane

Location, climate, nodal structure, and description of typical house plan

Ghardaia region (32.4° N, 3.8° E) is located 600 km from the coast, at an altitude of 450 m above sea level. It is influenced by a dry climate, characterized by very low precipitations (160 mm/year), very high temperatures in summer and low temperatures in winter (frosty from December to mid-February). The climate is hot and dry in the summer with temperatures variation between a maximum of around 45 °C and a minimum of 20 °C, thus giving a large diurnal temperature swing. Winter temperatures vary between a maximum of 24 °C and a minimum of 0 °C. Normal temperature in January is 10.4 °C and 36.3 °C in July. The average annual range is about 12.2° amplitudes of monthly average temperatures. They are more moderate in winter than in summer (average 11°C in winter and 13.5 °C in summer). The monthly maximum amplitudes are larger in summer than in winter fluctuates around 20 °C. Solar radiation is intense throughout the year with a maximum of 700 W/m^2 in winter and 1000 Wm^2 in summer, measured on the horizontal surface [20].

The study was carried out on a building in URAER, Ghardaia. Figure 1 is a schematic outline of apartment building; the apartment has a surface of 95.74 m^2 with a living space of 71.3 m^2, and wall heights are equal to 2.8 m. A given building is composed of a certain number of rooms, walls, doors, and also glass-windows. Layer thickness, composition and thermal transmittance values U for walls, ground and roof and glass thermal transmittance values are given in references [20-25]. In these works, the diagram and the solar path serve to identify the shade and particularly the influence of the shade of walls on the other opaque walls.

Therefore, the splitting up of the building into thermal zones induces the setting of nodes of temperature by zone. We have been induced to assign a type to each node. The nodes are concerned with different phenomena. In [16], we give the types of nodes encountered. For a given building, when the node structure is established, it is easy to fill up each element of the mathematical model. The structure will include six zones' numbers (fig. 1). Windows shall be designed to limit air leakage. The air infiltration rate shall not exceed 2.8 m^3/h per linear metre of sash crack when tested under a pressure differential of 75 Pa. For our study, we con-

Table 1. Layer yhickness, walls composition and *U* values for building envelope

	Composition	Thickness [cm]	*U* [Wm^{-2}K^{-1}]
Exterior walls	Mortar cement stone Mortar cement Coating plaster	1.5 40.0 1.5 1.0	1.97
Interior walls	Mortar cement stone Mortar cement Coating plaster	1.5 15 1.5 1.0	2.82
Ground	Tiling Cement Stone Concrete	2.5 1.0 6.0 24.0	0.93
Roof	Plaster Slab Mortar	1.5 12.0 3.0	1.05
Fial glass	Single pane, clear	0.2	5.91

sider that the window composition comprises in addition to the configuration given in tab. 1, wood blinds usually separated from the previous configuration by an air gap of 2 cm. We assume that the heat transfers through windows are only by conduction. However, the doors are made of wood with a thickness of 2 cm: $\lambda = 0.14$ W/mK, $\rho = 500$ kg/m^3, and $C_p = 2500$ J/kgK, where λ, ρ, and C_p are, thermal conductivity, density, and specific heat capacity, respectively.

Integration of the eave and their effect upon the temperature

Implementing the general law of building energy conservation, we arrive to a non stand alone system governed by one hundred and forty one non-linear ordinary differential equations. Subsequently, it is essential to implement numerical methods that compute these temperatures. Designed to solve such problems, Runge-Kutta fourth order numerical method was used to apprehend thermal behavior of walls and air subjected to varied solicitations. The elaborated interactive programs allowed a better understanding heat transfer phenomenon of walls and air under dynamic regime. Windows and black-out curtains remained closed all over the period. The instantaneous temperatures of air and wall surfaces were calculated by entering the measured meteorological data.

In a hot climate, it is essential to reduce the exposed wall surfaces to protect them from overheating in summer. So in integrating the shading device on the southern walls, we can significantly reduce temperatures. To show the advantage of the shading device we chose the days August 25 to 30, these days correspond to a completely clear sky and an ambient temperature between 24 and 42 °C. Wind velocity is between 0.25 and 10.2 m/s and the average relative humidity equal to 35%. The incident solar radiation (diffuse radiation) for a vertical plane facing south was determined using numerical models [26, 27]. Figure 2 gives an idea of the temperature profiles obtained by numerical simulation, and fig. 3 predicts the calculated specific humidity using the same conditions inside the sitting room for two different cases: if the habitat is in its original state and if the habitat is with the shading device. These results take into account the compactness index. The main impact of building compactness from the indoor climate point of view is its effect on the envelope's surface area, relative to the floor's area, or the space volume, and hence, the rate of heat exchange of the building with the outdoors. In hot dry climates, the surface volume area ratio should be as low as possible to minimize heat gain and the compactness is better when the compactness index is lower [16]. The first is the real or ordinary case when the house is exposed to the Sun at its four façades and compactness index equal to 0.5882. The second case corresponds to a row house, *i. e.*, when only the south and north façades are exposed $S/V = 0.2564$.

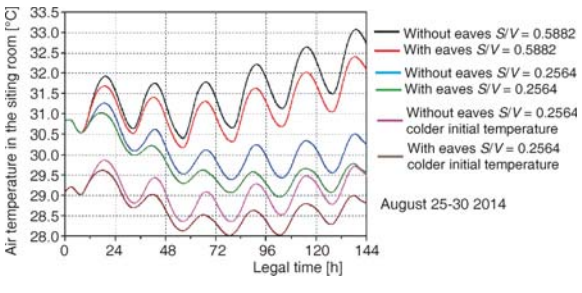

Figure 2. Sitting room temperatures

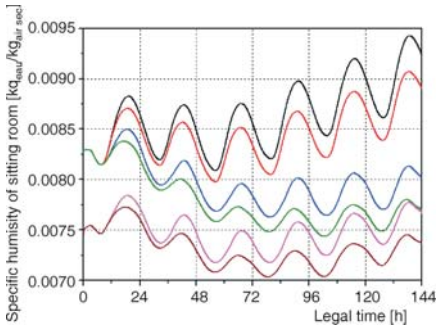

Figure 3. Specific humidity of sitting room

The most commonly used indicator of thermal comfort is air temperature, it is easy to use and most people can relate to it. But although it is an important indicator to take into account, air temperature alone is neither a valid nor an accurate indicator of thermal comfort. Air temperature should always be considered in relation to other environmental factors: radiant temperature, air velocity, and humidity. The advantage of our proposed model is that these four factors were taken into consideration. The present study demonstrates that the inclusion of the shading device (eaves) slightly reduced the temperature of sitting room. The difference maximum (1 °C) is at 19:45, and specific humidity follows the same scenario. Consequently, we can say that the integration of this architectural technique does not achieve thermal comfort since the internal temperatures are not reached. In winter the angle between the rays and the horizontal is less important in summer many winter rays pass under the eaves and reach the façade. While some summer rays reach the facade, they are stopped by shading devices.

Integration and effect of solar shading

The main function of a shading system is the protection of the building transparent envelope from solar radiation in summer conditions, so preventing overheating by blocking the access of unwanted energy flow into the building. Among the several shading solutions for limiting this thermal load, intercepting the solar radiation before it reaches the glazed area, through the use of external shading devices, is the most effective one [28]. We are interested in optimizing the length of the roof overhang. Figure 4 shows a detailed geometric description of this roof overhang. The incident radiation is reduced by shading, this can be explained by a radiation attenuation factor, which is the ratio of the shaded area and the total area of the glazing. For the direct radiation component, the attenuation factor F_B is calculated using the geometric laws that connect the shaded area O to the other parameters shown in fig. 4:

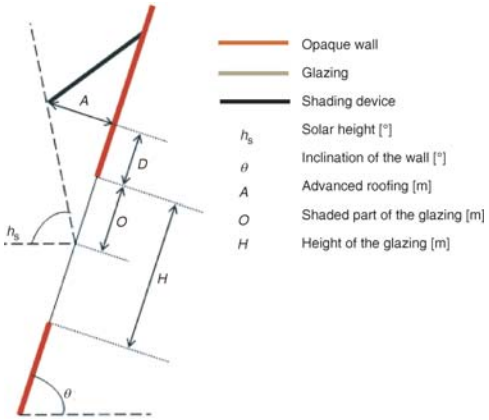

Figure 4. Integration of shading device

$$F_B = \frac{O}{H} \tag{18}$$

$$O = \frac{A\left(\tan(h_s) - \dfrac{1}{\tan\theta}\right)}{1 + \dfrac{\tan(h_s)}{\tan\theta}} - D \tag{19}$$

As a first approximation, the attenuation factor F_D of the diffuse radiation component can be calculated by taking the ratio between the angle at which the solar shading is seen from the windows, this according to the two main directions (zenith and azimuth).

$$F_D = \frac{\arctan\left(\dfrac{A}{(D + (H/2))}\right)}{\pi - \theta} + \frac{\pi - 2\theta}{2\pi - 2\theta} \tag{20}$$

If the sensor is semi-transparent, the masking effect is not the same compared to a completely opaque sensor. In this case, we must introduce a coefficient C_{ST} to take into account the semi-transparency of the masking effect. The new attenuation factor F'_B can be calculated:

$$F'_B = C_{ST} F_B = C_{ST} \frac{O}{H}, \quad C_{ST} = (1-\xi) + \tau_v \xi, \quad \xi = \frac{1 - S_{cel}}{S_{tot}} \tag{21}$$

From the expressions (19) and (21), the attenuation factor is calculated:

$$F'_B = \frac{C_{ST}}{H}\left[\frac{A\left(\tan(h_s) - \frac{1}{\tan\theta}\right)}{1 + \frac{\tan(h_s)}{\tan\theta}} - D\right] = \frac{1}{H}\left[\frac{C_{ST} A\left(\tan(h_s) - \frac{1}{\tan\theta}\right)}{1 + \frac{\tan(h_s)}{\tan\theta}} - C_{ST} D\right] \tag{22}$$

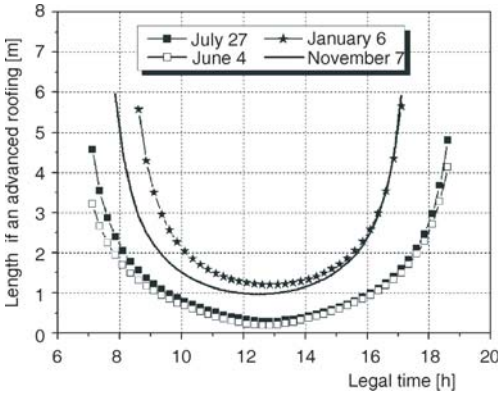

Figure 5. Length variation of the advanced roofing

The semi-transparent mask corresponding to an advanced roofing A, to an overhang D and to a coefficient C_{ST} is equivalent to an opaque mask of an advanced $A' = C_{ST} A$ (which is to remove the transparent part of the mask) and an overhang $D' = C_{ST} D$ (the overhang does not affect the opaque part of the mask). This study is valuable for opening and even for an opaque wall. For an opening, in our case: H = 0.9 m, O = 0.9 m, θ = 90°, and D = 0 m. Figure 5 shows four examples for two seasons (winter and summer), and this for a latitude corresponding to Ghardaia province. The calculations correspond to the horizontal advanced roofing that is fixed horizontally.

Moreover, according to the orientation, a vertical opening can be easily managed with respect to solar gain. In contrast, horizontal surfaces capture some energy in winter and bring overheating in summer.

The observed results certify that the total shading of the glazing is not provided throughout the day, especially just after sunrise and before sunset. It is necessary to insert advanced roofing *at sunrise* around 4.5 m and 3.2 m for selected days in months of June and July, respectively. For sunset, it is essential to include advanced roofing around 4.8 m and 4.1 m to ensure total shading solutions. This is not obvious for only one glazed surface area of (0.9 m × × 0.8 m). Heat transfer through openings depends on receiving surfaces and orientation. The advanced roofing can be designed to control the amount of the direct solar gain. The application of solar shading can reduce solar gain in summer reducing air-conditioning costs and allows solar heat gain in winter, thereby saving heating costs.

Conclusions

A new approach to modelling of multi-zone buildings in Saharan climate was introduced. Thermal nodal method was used to apprehend thermal behavior of air subjected to varied solicitations. The rate of heat exchange of the building with the outdoors. Proper use of

building geometry parameters will noticeably minimize building energy and improve the internal temperature of the building. The compactness of a building form is essential for the building energy status. In hot dry climates, the surface volume area ratio should be as low as possible to minimize heat gain and the compactness is better when the compactness index is lower. Heat gains through the walls are certainly the main cause of overheating of these habitat types. This Sun protection covers all the external walls of housing: roof, walls, and windows. This is an important step in the design of bioclimatic habitats. But, the realization of effective Sun protection is the second fundamental phases of the design of energy efficient housing.

The integration of a solar protection with a rectangular geometric shape at the south facing opening does not provide total shade especially at sunrise and sunset. For this reason it is recommended to think about the optimization of the geometry of the solar system and the opening and facade design.

Nomenclature

C_{as} – heat capacity of the air mass, [JKg^{-1}K^{-1}]
C_v – heat capacity at constant volume, [Jkg^{-1}K^{-1}]
CI_s, CI_L – internal sensitive and latent powers due to appliances, occupants, lighting, [W]
H_s, H_L – sensitive and latent enthalpy of the humid air, [J]
$H^e(i)$ – enthalpy of the humid air mass entering the Zone i, [J]
$H^{leav}(i)$ – enthalpy of the humid air mass leaving the Zone i, [J]
H_r – relative humidity, [%]
L_v – latent heat of vaporization of water, [Jkg^{-1}]
j – number of the inner surface (wall, door, and window) in Zone i
$NW(i)$ – total number of the interior surfaces (wall, door, and window) in Zone i
P_{sat} – pressure of saturation vapor, [Pa]
P_s, P_L – sensitive and latent powers provided by the air-conditioning, [W]
$Q_{mas}^{trans}{}_{(n,i)}$ – mass flow transiting from zone n to Zone i, [kgs]
$Q_{mas}^{trans}{}_{(n,i)}$ – mass flow of the dry air transiting from zone i to zone n, [kgs^{-1}]
$r_s(i)$ – specific humidity : mass of water vapor contained in the unit mass of dry air, [kg_{vap}/k_{gas}]
S – surface [m^2]
S_{cel} – the covered area [m^2]
S_{tot} – the total area [m^2]
$T_{al}(n)$ – air temperature of the Zone n = air temperature entering the Zone i, [K]
T_{sij}, T_A – temperature of surface j in Zone i, [K]

Greek symbols

τ_V – the transmission rate of the transparent part of the sensor
ξ – the semi-transparent sensor, equal to the ratio of the transparent area and the total

References

[1] Hong, T., Jiang, Yi., A New Multizone Model for the Simulation of Building Thermal Performance, *Building and Environnement, 32* (1997), 2. pp. 123-128
[2] Stephenson, D. G., Mitalas, G. P., Calculation of Heat Conduction Transfer Functions for Multilayer Slabs, *ASHRAE Transactions, 77* (1971), 2, p. 117
[3] Stephenson, D. G., Mitalas, G. P., Room Thermal Response Factors, *ASHRAE Transactions, 73* (1967), 1, pp. 1-10
[4] Laret, L., *et al*., Building Specification, IEA Annex 10 report, University of Liege, Liege, Belgium, 1988
[5] Jiang, Y., State Space Method for Analysis of the Thermal Behaviour of Rooms and Calculation of Air-Conditioning Load, *ASHRAE Transactions, 88* (1981), 2, pp. 122-132
[6] ***, *SIMBAD Building and HVAC*, Toolbox, Version 3.1, CSTB, France, 2003
[7] Fanger, O. P., *Thermal Comfort*, McGraw Hill, New York, USA, 1973
[8] Larsen, S. F., *et al*., Thermal Behavior of Building Walls in Summer: Comparison of Available Analytical Methods and Experimental Results for a Case Study, *Building Simulation*, *2* (2009), 1, pp. 3-18, DOI 10.1007/S12273-009-9103-6
[9] Cartes, I. A., Traditional Architecture, Building Materials and Appropriate Modernity in Chilean Cities, *Renewable Energy, 15* (1998), 1-4, pp. 283-286

[10] Monsen, W. A., *et al.*, Prediction of Direct Gain Solar Heating System Performance, *Solar Energy, 7* (1981), 2, pp. 143-147
[11] Saulnier, J. B., Alexandre, A., Heat Transfer Modeling by the Nodal Method: Its Principles, Successes and Limitations (in French), *Revue Generale de Thermique, 280* (1985), pp. 363-372
[12] Auger, J. L., *et al.*, Operation of Solar Collector in Dymanic Regime (in French), *Revue Generale de Thermique, 239* (1981), pp. 81 l-824
[13] Chapman, A. J., *Heat Transfer*, Macmillan, New York, USA, 1984
[14] Roux, J. J., Thermal Behavior of Buildings (in French), Institut National des Sciences Appliquees, Departement De Genie Civil, INSA de Lyon, France, 2000
[15] Jannot, Y., *Heat Transfer* (in French), Ecole des Mines, Nancy, France, 2012
[16] Bekkouche, S. M. A., *et al*., Influence of the Compactness Index to Increase the Internal Temperature of a Building in Saharan Climate, *Energy and Buildings, 66* (2013), Nov., pp. 678-687
[17] ***, http://en.wikipedia.org/wiki/Enthalpy
[18] Nadeau, J.-P., Puiggali, J.-R., *Drying-Physical Processes to Industrial Processes*, Tec & Doc-Lavoisier, 1995 (ISBN 2-7430-0018-X)
[19] Rumianowski, P., *et al*., An Adapted Model for Simulation of the Interaction between a Wall and the Building Heating System, *Proceedings*, Thermal Performance of the Exterior Envelopes of Buildings, IV Conference, Orlando, Fla., USA, 1989, pp. 224-233
[20] Bekkouche, S. M. A., Thermal Resistances of Local Building Materials and their Effect Upon the Interior Temperatures Case of a Building Located in Ghardaia Region, *Construction and Building Materials, 52* (2014), Feb., pp. 59-70
[21] Hamdani, M., *et al*., A New Modelling Approach of a Multizone Building to Assess the Influence of Building Orientation in Saharan Climate, *Thermal Science*, 2014, doi: 10.2298/TSCI131217026H
[22] Bekkouche, S. M. A., *et al*., Influence of Building Orientation on Internal Temperature in Saharan Climates, Building Located in Ghardaia Region (Algeria), *Thermal Science, 17* (2013), 2, pp. 349-364
[23] Bekkouche, S. M. A., *et al*., Introduction to Control of Solar Gain and Internal Temperatures by Thermal Insulation, Proper Orientation and Eaves, *Energy and Buildings, 43* (2011), 9, pp. 2414-2421
[24] Bekkouche, S. M. A., Benouaz, T., Cheknane, A., A Modelling Approach of Thermal Insulation Applied to a Saharan Building, *Thermal Science, 13* (2009), 4, pp. 233-244
[25] Bekkouche, S. M. A., Modelling of Thermal Behavior Some Solar Devices (in French), Ph. D. thesis, University Abou Bekr Belkaid, Tlemcen, Algeria, 2009
[26] Yaiche, M. R., Bekkouche, S. M. A., Conception and Validation of an Excel Program to Estimate the Solar Radiation Incident in Algeria in the Case of a Totally Clear Sky (in French), *Revue des Energies Renouvelables, 11* (2008), 3. pp. 423-436
[27] Yaiche, M. R., *et al*., Revised Solar Maps of Algeria Based on Sunshine Duration, *Elsevier Energy Conversion and Management, 82* (2014), June, pp. 114-123
[28] Bellia, L., *et al*., Effects of Solar Shading Devices on Energy Requirements of Standalone Office Buildings for Italian Climates, *Applied Thermal Engineering, 54* (2013), 1, pp. 190-201

Paper submitted: April 12, 2014
Paper revised: September 3, 2014
Paper accepted: September 8, 2014